# CAPTURING THE IRRIGATION DYNAMICS AT FIELD SCALE IN A RICE DOMINATED BASIN USING SATELLITE REMOTE SENSING

Kirthiga S.M[1], Narasimhan B[2] and C.Balaji[3]

## ABSTRACT

Monitoring the dynamics of Indian agriculture is challenging due to small field sizes and heterogeneity in management practices. The global availability of high resolution remote sensing data at multi-spectral and multi-temporal ranges have helped in increasing its usage for monitoring of natural resources in developing nations. This study explores the possibility of using an integrated approach combining high resolution images from Sentinel and Landsat missions to capture the irrigation dynamics at field scale. A part of the rice paddy dominated Tamirabharani basin (southern parts of south India), which was considered for the study is posed with serious challenges from cloud cover throughout the year. Thus, integrated use of optical and microwave remote sensing was attempted in the study. The irrigated rice paddy fields were classified at high resolution (20m) using a cloud free Sentinel-2 image with ancillary information from Sentinel-1 time series, Landsat-8 time series and ALOS Global Digital Surface Model data. Supervised classification using Random forest classifier was performed for the identified 10 land-use classes. The classification procedure was validated against ground truth data and gave an overall accuracy of 79.6%. The classification accuracy for rice paddy was relatively higher with producer's accuracy of 88% (F score of 86%).The field scale variability has been adequately captured. About 94% of the classified rice paddy matched with irrigated land cover from the Global irrigated area map (GIAM) datasets which confirm the spatial consistency of the method. The whole algorithm was implemented in Google Earth Engine (GEE) cloud computing platform reducing the processing time and local storage needs. The results are promising and in view of above the use of the procedure at regional level is suggested. An attempt to further capture the irrigation dynamics at 12-day interval for the classified rice paddy fields was attempted with the backscatter values from Sentinel-1 time series data and field collected irrigation frequency data.

**Keywords:** Irrigated crop mapping, Google Earth Engine, Sentinel -1, Sentinel-2, Landsat-8.

## 1. INTRODUCTION

Irrigated agriculture is a major thrust area to ensure food security since it contributes to 40% of global food production (FAO, 2012). Globally, an average of 7,700 cubic meter of water per hectare is used annually for irrigation purposes, with the withdrawals highly varying across space and time. The present irrigation water use efficiency is around 56%, largely varying from 23% in water abundant regions to 72% in water scarce areas. Growing water scarcity and changing climate regimes calls for continuous monitoring of irrigated agriculture to capture the spatial and temporal dynamics.

[1] PhD Research Scholar, Indian Institute of Technology, Madras (IITM). Chennai 600036, India; E-mail: smkirthiga@gmail.com

[2] Professor, Envi. and Water Res. Engg. Division, Indian Institute of Technology, Madras (IITM). Chennai 600036, India; E-mail: nbalaji@iitm.ac.in

[3] Professor, Mechanical Engineering, Indian Institute of Technology, Madras (IITM). Chennai 600036, India; E-mail: balaji@iitm.ac.in

Remote sensing technology had been widely used in the past decade for mapping irrigated regions across globe enabling region-wide water management. Available studies range from using images acquired byoptical sensors to radars, through a variety of approaches spanning from using single sensor/single date imagery to using multi-sensor/multi-date imageries to capture irrigated crop classes at various spatial scales (Ozdogan et al. 2010).

Most of the earlier studies used single date multi-band image from optical sensors or their derivatives like Normalized Difference Vegetation Index (NDVI) to identify irrigated crops (Ozdogan et al. 2010). Popular approach had been to use multi-temporal images to distinguish between land cover classes based on their phenology which is highly relevant for vegetative land-use types (Thenkabail et al. 2005). The fine spatial resolution satellites like Landsat have longer revisit periods, while the highly frequent satellites like Moderate Resolution Imaging Spectroradiometer (MODIS) which is appropriate to capture the crop phenology, have coarser spatial resolution.

Thus, researches have suggested the use of multi-sensor data by merging the information across sensors, to improve the spatial resolution (Ozdogan et al. 2010). However, the problem of cloud interference is persistent in optical sensors,encouraging the use of microwave imageries to segregate the land cover classes across space and time. Sentinel-1 microwave sensor provides imageries with high spatial and temporal resolution. Usage of the microwave images for crop mapping is becoming quite popular since it is highly suitable for tropical, developing countries like India, where continuous cloud cover, small field sizes and heterogeneity in farming practices are prevalent (Singha et al. 2019). However, the lone use of single-date or multi-date microwave imagery introduces salt and pepper noise effect in the resultant classes and thus needs to be combined with high resolution optical sensors to the demarcate land-use boundaries realistically (Zhang et al. 2018).

With this background, a hybrid approach combining multi-sensor data, is attempted in the current study to map rice paddy. The common rice paddy cultivation is heavily driven by irrigation and requires about 5-7 cm layer of standing water throughout its peak vegetative phase (FAO, 2012). The study area, a part of Tamirabharani basin which is located in southern parts of Tamilnadu located in South India. It is dominated by rice paddy cultivation. With rice paddy grown during two main seasons (Kar and Pishanam), the agricultural water demand for a year is approximately about 2645 Million Cubic Meters (MCM) while the current water potential is only about 2119 MCM per year, already facing deficit conditions (Palanisami et al. 2011).

Thus, the main objective of the study is to map rice paddy cultivations dynamically for a given year (here, 2017-18) to help in continuous monitoring of water balance for the basin. To accomplish the above-mentioned objective, 20-m resolution Sentinel-2 median imagery from images covering the months of February and March, 2018 with no cloud cover is selected as the anchor image. Ancillary information from metric composites derived from time series images ofLandsat-8 Enhanced Vegetation Index (EVI) data, Sentinel-1 C-Band microwave data for the year 2017-18 and ALOS Global Digital Surface Model (DSM) data based elevation and slope values are used in the classification procedure. Random Forest classifier is used to learn from the training pixels (472 pixels) and subsequently classify the image. A set of random 225 pixels are used for validation purposes. In addition, the time-series data of the microwave sensor (Sentinel-1 C-band) for the years 2017-18 are analysed for understanding the ability of the sensor signals to capture the irrigation frequency in the rice-paddy fields.

## 2. MATERIALS AND METHODS

### 2.1 Study Area – Gadana Basin

A part of Tamirabharani basin (one of the major perennial river basin in Tamilnadu, India), the gadananadhi (known as gadana) sub-basin is chosen to implement and test the proposed methodology. The location of the sub-basin is shown in Figure 1. The gadana basin covers about 866 sq. km and is dominated by rice paddy cultivation. Located near the Western Ghats, the annual rainfall is about 680 mm. The rainfall is mainly received during North-East monsoon (61%), while South-West monsoon (16%) and summer rains (13%) also contribute considerably. Thus, the study area is clouded most of the time in the year. Rice paddy is cultivated predominantly during two main seasons, the Kar season (June to September) and the Pishanam season (October to February). The region belongs to highly irrigated zones in the country with irrigation water sources from both canal and groundwater wells.

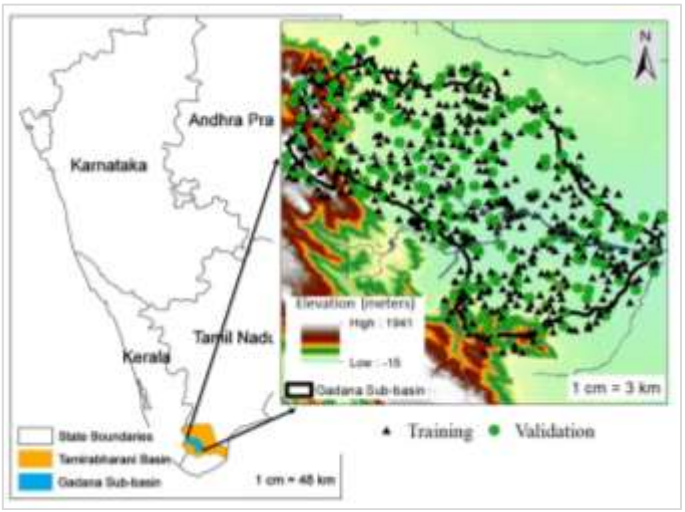


**Figure 1.** Map showing the location of the study area. Inset map showing the gadana sub-basin with elevation values in the background along with sample points used for training and validation.

### 2.2 Platform and Datasets

Google Earth Engine (GEE) (Gorelick et al. 2017) is a cloud computing platform where various publically accessible datasets are readily available to the users. Highly functional interactive coding platform (using JavaScript) is provided to access, process, analyse and infer from the datasets. Thus, GEE drastically minimizes local storage needs, download and computational time.

Sentinel-2 is an optical sensor with 13 bands having 10-20 metre spatial resolution and a temporal resolution of 5-10 days (available from June, 2015 till present). Level-1C data representing the Top of Atmosphere (TOA) reflectance is used in the study. Sentinel-1 products are from Synthetic Aperture Radar (SAR), a dual-polarized instrument working in C-band (5.405GHz) region. The image collections contains Ground Range Detected (GRD) images. The pre-processing includes thermal noise removal, radiometric calibration and ortho-correction using Digital Elevation Models (DEM) (pre-processed using Sentinel-1 toolbox).

The Interferometric Wide Swath (IW) mode of image collection is preferred since it is specially designated for capturing land surfaces and gives consistent images across years (available from 2015 till present). The spatial resolution is 10 metre (resampled) and temporal resolution is about 12 days. Enhanced Vegetation Index calculated from Near Infra-Red (NIR), Red and Blue bands of Landsat-8 mission (30 metre resolution, 16-day frequency and available from 2013 till present)is used in the study to precisely demarcate vegetation classes from non-vegetation classes. Recent version of Digital Surface Model (DSM) from ALOS (World 3D Topographic Data)is available at 30 metre resolution. The elevation and slope derivatives from ALOS are utilized in the study to particularly differentiate between forest and crop classes. CHIRPS Daily data (Climate Hazards Group InfraRed Precipitation with Station Data) which is available at 0.05 degree resolution (available from 1981 till present). It incorporates satellite data assimilated with in-situ station data and is a popularly used for precipitation pattern analysis across world. The CHIRPS data is used in the study, to analyse the rainfall patterns in the study region.

## 3. Methodology

### 3.1 Image Pre-Processing

Anchor image is selected as median of the Sentinel-2 (Level 1C) images which has less than 1% cloud cover for the year 2018. Of the 70 scenes (for whole of 2018), only three images obtained in the months of February and March, 2018 satisfied the given criteria (cloud cover < 1%) and are used to compute the anchor image. Sentinel 1 is chosen as the master image since it has high spatial resolution (~10 metre) and can capture the sharp boundaries of rice paddy at field scale. However, the images from peak crop growing seasons was not available due to cloud noise and thus, supplementary information from other sensors are used to accurately map the current year's rice paddy extent.

Sentinel-1 images acquired with vertical transmit and vertical receive (VV) and vertical transmit and horizontal receive (VH) polarizations are selected. Earlier studies have shown that VV polarisation is sensitive to soil moisture variations while VH is sensitive to volume scattering of vegetative canopy (Zhang et al. 2018). Since mapping of rice-paddy (which has both canopy cover and standing water) is the major objective, both the polarizations are considered. A total of 77 scenes in each polarization was available. Speckle filtering technique with box kernel (3x3 window) is applied on the images to smoothen and remove the speckle effect. Direct usage of the time-series of Sentinel-1 images in the supervised classifier consumed huge processing time for training and did not improve the performance of the algorithm. Thus, the mean metric is selected as it provided better segregation between the 10 land-use classes consuming lesser computational time. In addition, another metric derived from Sentinel-1 is proposed in the study. The study area contained numerous small tanks and these tanks had been alternatively wet and dry across the years. Thus, those regions are highly mixing with other classes, especially the rice paddy. To handle this and to better segment the waterbodies, seasonal differencing of the SAR images is performed. CHRIPS rainfall data was used to analyse the continuous wet days and dry days. The median image of the wet period (20 Aug, 2018 to 30 Aug, 2018) is differenced with the median image of the dry period (1 April, 2018 to 30 April, 2018). The resultant images from both the polarizations are added as an ancillary layer to the classifier.

Landsat-8 images are atmospherically corrected and the pixels values represent the surface reflectance. Thus, the images might be able to capture the land-use pattern more realistically when compared to the TOA reflectance from Sentinel-2. The median values of Landsat EVI time-series data for the years 2017-18 is considered in

the classification procedure. Using the median metric is found to be more meaningful than using the whole time-series since the data had lot of artificial spikes in the temporal profile due to the presence of clouds.

### 3.2 Supervised Classification

Random Forest (RF) classifier performs pixel-based supervised classification. The classifier uses bagging approach (with replacement) to form ensemble of decision trees by random sampling from training data. The correlation between the trees is reduced by optimal splitting of the nodes which is done iteratively until the pixel is assigned to a class. The RF classifier also performs cross-validation internally by using two-thirds of samples for training and the remaining samples for validation. Two major parameters are required for the classifier, the number of decision trees (Ntree) and the number of variables (Mtry) used for dividing the trees.

In the study, 17 variables (derived from Sentinel-1 and 2, Landsat-8 and ALOS data) are utilized to perform the classification. A total of 472 sample points generated randomly and labelled manually with the help of Google Earth high resolution images are used for training (Figure 1). The classifier has been trained to capture the ten land-use types namely Closed Canopy Forest (CCF), Open Canopy Forest (OCF), Grassland, Urban, Plantation, Waterbodies, Barren, Other crops, Rice paddy and Sugarcane. It was made certain that each class was represented by a minimum of 30 sample training points. After a series of trial and error approach, Ntree is set to 40 and Mtry to default (square root of input variables).

### 3.3 Analysis of Sentinel-1 Time-Series

The classified rice paddy are masked in the Sentinel-1 time series and the histogram of backscatter values for every classes are analysed. The temporal variation of backscatter values of the selected fields is extracted and compared with field observed irrigation frequency data for hidden patterns. This analysis is designed to test the feasibility of microwave imagery in detecting irrigation signals to further help in water management.

### 3.4 Validation

Random points are generated across the study area and google earth high resolution imagery was used to identify the present land-use types. A set of 225 sample points with a minimum of 10 samples per class is selected for validation (Figure 1). Confusion matrix is generated after comparison between the classified image and validation points. Statistics like overall Accuracy and kappa coefficient are calculated and the performance of the method is assessed. The effectiveness of the algorithm to capture land-use types is quantified using Producer's accuracy (accuracy of the algorithm), User's accuracy (reliability of the algorithm) and F score (measure of preciseness and recall capability)(description available in Zhang et al. 2018).

To test the spatial consistency of the classified rice paddy, the classified image is compared with the widely used Global irrigated area map (GIAM) datasets at a resolution of ~500 metre.

## 4. RESULTS AND DISCUSSION

### 4.1 Accuracy Assessment for The Land-Use Types

The separability of the land-use classes under each variable is shown in Figure 2.

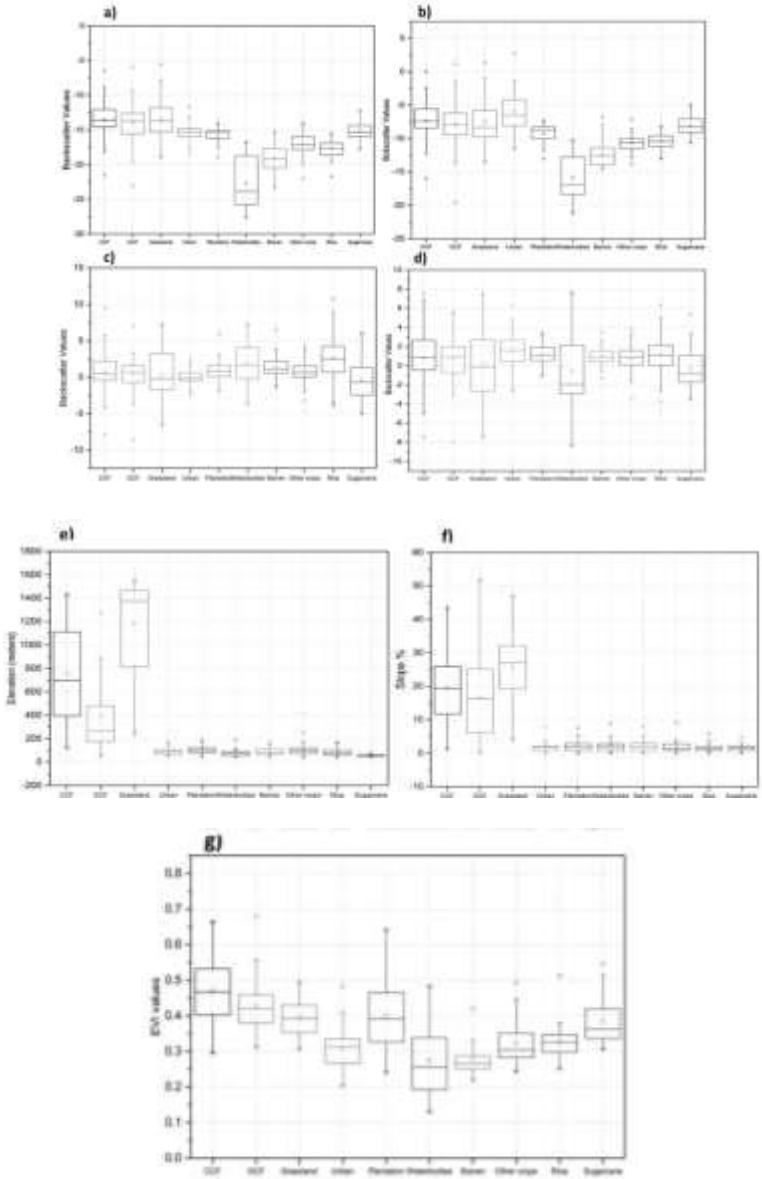


**Figure 2.** Box plots representing the value spread of each variable used in the classifier across all the land-use types. a) Mean of VH time-series b) Mean of VV time-series c) Seasonal differenced VH d) Seasonal differenced VV e) Elevation f) Slope and g) EVI. The box denotes the 25-75 percentile spread of data with small square marker denoting the mean, the whiskers represent the outliers while the crosshairs represent the 99-1 percentile spread. The land-use types are arranged in order viz. Closed Canopy Forest (CCF), Open Canopy Forest (OCF), Grassland, Urban, Plantation, Waterbodies, Barren, Other crops, Rice paddy and Sugarcane.

From the Figure 2a and 2b it is seen that mean image from the time-series of Sentinel-1 VH and VV polarization is able to capture the variability between most of the classes. The forest types show relatively higher backscatter values in VH mean image due to volume scattering and thus, are well separated from the other land-use types. Water body is noticed to have highest uncertainty in both VH and VV mean images. This could be attributed to the nature of water bodies in the study area, highly fluctuating within a given year. The mean VH and VV images are able to segregate non-vegetation classes like urban and barren. The separation of non-agricultural vegetative classes (forest and grassland) from agricultural classes (rice paddy, other crops) is very evident using the mean VH and VV images. In addition, the sugarcane is well separated from rice-paddy. However, variability within the some agricultural classes (other crops and rice-paddy) or within the non-agricultural classes is not highlighted in the mean SAR images. Furthermore, sugarcane and plantation classes are showing similar distribution of values since both are dominated by volume scattering.

The box plots of seasonal differenced VH and VV are given in Figure 2c and 2d. Very less variability between classes is observed. However, urban, barren and plantation classes show very less spread of values and the mean is concentrated around zero. This exactly captured the invariable nature of those land-use types within the year and thus, improved the accuracy of classification of those classes. The other-crops category also showed similar behaviour since they are short duration crops and cultivation of those crops will not fall during the wet or dry period that is selected in the study.

Water body and grassland categories recorded the highest variability. As discussed earlier, the water bodies are highly fluctuating and thus gave highest deviation between dry and wet periods. Grasslands also flourish during the wet period while they degrade during the dry period. The classification of land-uses viz. rice-paddy, sugarcane, closed and open canopy forests did not improve much with this ancillary product (season differencing of VH and VV). However, the mixing of other categories with the above-mentioned classes are highly reduced.

The box plots of elevation and slope (Figure 2e and 2f) show definite advantage for forest and grassland classes. The Closed canopy forest and Open canopy forest is segregated well with elevation than any other ancillary products selected in the study. The EVI values largely help in capturing the internal variability amongst the vegetation classes (Figure 2g). The crops and forest classes are well differentiated with definite mean EVI values.

Table 1 gives the overall accuracy metrics of the classification procedure. The overall accuracy is 79.6% and kappa statistic is about 0.77. F score is high for the urban, grassland and rice paddy classes. Use of the hybrid approach proposed in the study has evidently helped in improving the accuracy of the classes. Highest producer's accuracy is obtained for CCF, Rice paddy, barren and sugarcane land-use types. The highest user's accuracy is obtained for urban, water bodies and grassland categories. The omission errors (error due to omitting of reference classes, complementary to producer's accuracy) are high in classification of OCF, Waterbodies and Plantation. OCF is largely confused only with CCF.

As discussed earlier, only elevation attribute gives clear demarcation between CCF and OCF. A few of the water bodies are confused/misclassified as rice paddy by the algorithm. This is inherently due to the fluctuating nature of most of the waterbodies in the study region. As mentioned earlier, the waterbodies have lot of uncertainty showing a larger value spread across all the attributes used in the procedure. Nevertheless, no other classes is confused for waterbody and thus 100% user's

accuracy is obtained. A few of the plantation land-use is misclassified as OCF which is due to the physical similarity between the classes. Inferior user's accuracy (high commission errors) is noticed in OCF, CCF, Barren and Plantation.

**Table 1.** Accuracy metrics of the land-use classes

| Classes | User's Accuracy | Producer's Accuracy | F score |
|---|---|---|---|
| CCF | 68% | 90% | 78% |
| OCF | 57% | 60% | 59% |
| Grassland | 100% | 80% | 89% |
| Urban | 100% | 85% | 92% |
| Plantation | 73% | 69% | 71% |
| Waterbodies | 100% | 67% | 80% |
| Barren | 70% | 88% | 78% |
| Other Crops | 91% | 77% | 83% |
| Rice-paddy | 85% | 88% | 86% |
| Sugarcane | 78% | 88% | 82% |

### 4.2 Classification of Rice Paddy

Rice paddy is well segregated having producer's accuracy of 88%, user's accuracy of 85% and F score of 86%. About 3 sample points are misclassified as sugarcane and 2 sample points are confused as barren of all the 40 sample points used for rice paddy validation. A few of rice paddy pixels are wrongly committed as waterbody and other crops category during the classification causing commission errors. However, the errors are minimal and the F score is 86% confirming the precision and recall capability of the proposed procedure in capturing rice paddy.

To validate the spatial consistency, classified rice paddy is compared with GIAM data. About 94% of rice paddy belonged to the irrigated classes of GIAM data. Around 27% of classified rice paddy belonged to Irrigated, conjunctive use, double crop class; 19 % belonged to Irrigated, conjunctive use, single crop; 16 % under the Irrigated, surface water, double crop; 10% is contained in Irrigated, surface water, single crop classes. In addition, due to the coarser nature, GIAM had some errors due to missing out of rice-paddy or misclassification which is highly reduced using the proposed method (Figure 3). This comparison strengthens the overall confidence on the suggested procedure.

### 4.3 Irrigation Dynamics

The classified rice paddy pixels have then been used to analyse the time series of VH and VV products of Sentinel-1 with an objective to detect irrigation signals from the temporal profile. The VV temporal profile is found to be highly sensitive to water and thus used for examination. Figure 4a and 4b shows the temporal profile of VV time-series in upstream and downstream rice paddy fields. Figure 4c gives the histogram of pure rice paddy field derived from Sentinel 1 VV polarization across the years 2015-2018.The histogram (Figure 4c) shows that the pure rice paddy field has a high frequency of VV backscatter values in range of -11 to -8 dB.The left tail region (-18 to -14 dB) matches well with the ponded conditions during the transplanting stages (agrees with Singha et al. 2019). From this inference, the transplanting dates (Pisanam season 2017-18) are marked in Figure 4a and 4b.

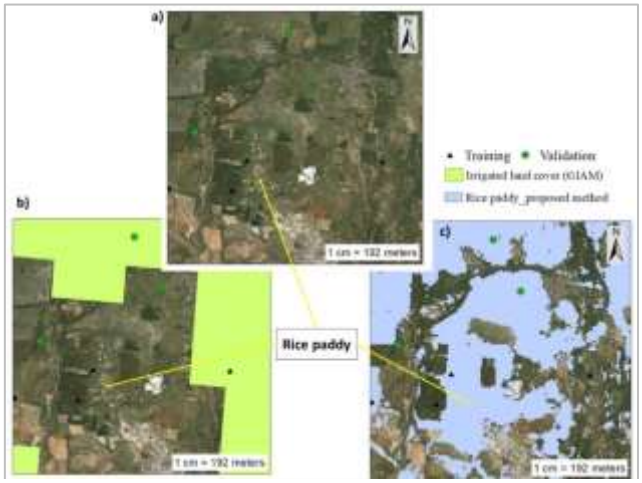


**Figure 3.** Comparison with GIAM data. a) Google earth image of a sample site b) Irrigated map from GIAM for same sample site c) Rice paddy map for the same site. The fine resolution of the proposed methodology clearly capturs the field scale variability in the rice paddy cultivation. Furthermore, the sugarcane and urban pixels are segregated and do not mix with rice paddy. This demonstrates the superiority of the method.

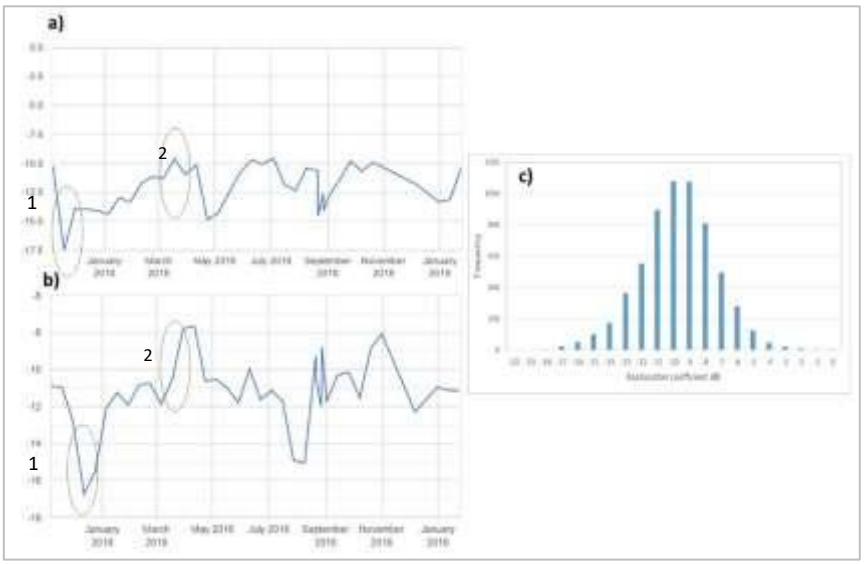


**Figure 4.** Plots derived from Sentinel-1 VV time-series data. a) Temporal plot of VV for upstream rice paddy field (X-axis →Date; Y-axis → Backscatter coefficient dB) b) Temporal plot of VV for downstream rice paddy field (X-axis →Date; Y-axis → Backscatter coefficient d B) c) Histogram of VV data for pure rice paddy field across years 2015-18. The inset oval marks the potential transplanting dates (1) and maturity dates (2) of the rice paddy crop for Pishanam season 2017-18.

The upstream rice paddy field has timely access to the irrigation water and is reflected from early transplantation date as marked in Figure 4a. This matched well with the in-situ field observation data. The downstream field has a slightly delayed transplanting date due to the time taken for water to reach the downstream. When the rice plant becomes matured, the canopy based volume scattering dominates and the

irrigation water requirement is also reduced. Thus, the backscatter values in VV polarization tend to increase post vegetative phase. This pattern is reflected in the time-series data where early March 2018 for upstream and mid-March 2018 for downstream fields are seen to have increasing backscatter values (Figure 4a and 4b). The small spikes within the transplanting dates and the harvesting dates might correspond to irrigation signals or depth of standing water versus the canopy cover. However, intense field comparisons will be required to make stronger conclusions about this.

## 5. CONCLUSIONS

A genuine technique based on Random Forest classifier using four different sensor data was developed to classify rice paddy in rice-dominated basin of India. The novel metrics which showed high ability to distinguish between classes were used in the classification procedure rather than the whole time series. The algorithm was implemented in Google Earth Engine and thus the procedure can be expanded to regional levels. A small explorative study to understand the potential of Sentinel-1 time-series to capture the irrigation dynamics was also performed.

Since the algorithm is dependent on the microwave data, the speckle effect in the classified image is visible. Thus, advanced image segmentation techniques can be applied on optical imagery and merged with the results to realistically represent the land-use boundaries. The seasonal composites of microwave imageries might have more information on agricultural land-use and should be explored when the region of interest has different crop species. Advanced techniques like Principal Component Analysis (PCA) can be performed on seasonal time-series data to improve the classification accuracy. While using the microwave imagery for exploring irrigation dynamics, the effect of precipitation should be considered. Future scope of the work will focus on developing strategies to capture irrigation dynamics by comparison with in-situ data.

## 6. REFERENCES

FAO, 2012. Facts available at http://www.fao.org.

Gorelick, N., et al. 2017 Google Earth Engine: Planetary-scale geospatial analysis for everyone. Remote Sensing of Environment 202, 18–27.

Ozdogan, M., Yang, Y., Allez, G.& Cervantes, C., 2010 Remote sensing of irrigated agriculture: opportunities and challenges. Remote Sens. 2 (9), 2274–2304. https://doi.org/10.3390/rs2092274.

Palanisami, K., Ranganathan, C.R., Vidhyavathi, A., Rajkumar, M. &Ajjan, N., 2011 “Performance of agriculture in river basins of Tamil Nadu in the last three decades – A total factor productivity approach”, Research report submitted to Planning Commission, Government of India, New Delhi, available at: http://planningcommission.nic.in/reports/sereport/ser/ser_river1905.pdf.

Singha, M., Dong, J., Zhang, G.& Xiao, X., 2019 High resolution paddy rice maps in cloud-prone Bangladesh and Northeast India using Sentinel-1 data. Scientific Data. 26 (6). https://doi.org/10.1038/s41597-019-0036-3.

Thenkabai,l P.S., Schull, M.&Turral, H. 2005 Ganges and Indus river basin Land Use/Land Cover (LULC) and irrigated area mapping using continuous streams of MODIS data. Remote Sensing of Environment. 2005;95(3):317–341. https://hdl.handle.net/10568/41039.

Zhang, X., Wu, B., Ponce-Campos, G., Zhang, M., Chang, S.& Tian, F. 2018 Mapping up-to-Date Paddy Rice Extent at 10 M Resolution in China through the Integration of Optical and Synthetic Aperture Radar Images. Remote Sens. 2018, 10, 1200. https://doi.org/10.3390/rs10081200.